TABLE A-1
Total Spillover Values for Different Region of Interest Geometry and Wall Thickness (FWHM = 10 mm)

Spillover value	Wall thickness		
	6 mm	10 mm	14 mm
Centered ROI (width = 4mm)	0.50	0.26	0.11
Full wall ROI	0.51	0.34	0.18

Further details for the one-dimensional and two-dimensional geometries can be found in Gambhir (*5*).

REFERENCES

1. Hutchins GD, Schwaiger M, Rosenspire KC, Krivokapich J, Schelbert H, Kuhl DE. Noninvasive quantification of regional blood flow in the human heart using ^{13}N ammonia and dynamic positron emission tomographic imaging. *J Am Coll Cardiol* 1990;15:1032–1042.
2. Muzik O, Beanlands RSB, Hutchins GD, Mangner TJ, Nguyen N, Schwaiger M. Validation of nitrogen-13-ammonia tracer kinetic model for quantification of myocardial blood flow using PET. *J Nucl Med* 1993;34:83–91.
3. Nitzsche EU, Choi Y, Czernin J, Hoh CK, Huang SC, Schelbert HR. Noninvasive quantification of myocardial blood flow in humans. A direct comparison of the [^{13}N]ammonia and the [^{15}O]water techniques. *Circulation* 1996;93:2000–2006.
4. Czernin J, Müller P, Chan S, et al. Influence of age and hemodynamics on myocardial blood flow and flow reserve. *Circulation* 1993;88:62–69.
5. Gambhir SS. Quantitation of the physical factors affecting the tracer kinetic modeling of cardiac positron emission tomography data [PhD thesis]. Los Angeles: University of California at Los Angeles; 1990.
6. Henze E, Huang SC, Ratib O, Hoffman EJ, Phelps ME, Schelbert HR. Measurement of regional tissue and blood-pool radiotracer concentrations from serial tomographic images of the heart. *J Nucl Med* 1983;24:987–996.
7. Iida H, Takahashi A, Tamura Y, Ono Y, Lammertsma A. Myocardial blood flow: comparison of oxygen-15-water bolus injection, slow infusion and oxygen-15-carbon dioxide slow inhalation. *J Nucl Med* 1995;36:78–85.
8. Krivokapich J, Smith GT, Huang SC, et al. Nitrogen-13-ammonia myocardial imaging at rest and with exercise in normal volunteers: quantification of absolute myocardial perfusion with dynamic positron emission tomography. *Circulation* 1989;80:1328–1337.
9. Frank JS, Langer GA. The myocardial interstitium: its structure and its role in ionic exchange. *J Cell Biol* 1974;60:586–601.
10. Zierler KL. *Circulation times and the theory of indicator-dilution methods for determining blood flow and volume.* Baltimore: Waverly Press; 1962:585–615.
11. Iida H, Kanno I, Miura S, Murakami M, Takahashi K, Uemura K. Error analysis of a quantitative cerebral blood flow measurement using $H_2{}^{15}O$ autoradiography and positron emission tomography, with respect to the dispersion of the input function. *J Cereb Blood Flow Metab* 1986:536–545.
12. Meyer E. Simultaneous correction for tracer arrival delay and dispersion in CBF measurements by the $H_2{}^{15}O$ autoradiographic method and dynamic PET. *J Nucl Med* 1989;30:1069–1078.
13. Smith GT, Huang SC, Nienaber CA, Krivokapich J, Schelbert HR. Noninvasive quantification of regional myocardial blood flow with ^{13}N ammonia and dynamic PET [Abstract]. *J Nucl Med* 1988;29:940.
14. Kuhle W, Porenta G, Huang SC, et al. Quantitation of regional myocardial blood flow using ^{13}N-ammonia and reoriented dynamic positron emission tomographic imaging. *Circulation* 1992;86:1004–1017.
15. Spinks TJ, Jones T, Gilardi MC, Heather JD. Physical performance of the latest generation of commercial positron scanner. *Trans Nucl Sci* 1988;35:721–725.
16. Kuhle W, Porenta G, Huang SC, Phelps M, Schelbert H. Issues in the quantitation of reoriented cardiac PET images. *J Nucl Med* 1992;33:1235–1242.
17. Porenta G, Kuhle W, Czernin J, et al. Validation of PET-acquired functions for cardiac studies. *J Nucl Med* 1988;29:241–247.
19. Gambhir SS, Schwaiger M, Huang SC, et al. Simple noninvasive quantification method for measuring myocardial glucose utilization in humans employing positron emission tomography and fluorine-18-deoxyglucose. *J Nucl Med* 1989;30:359–366.
20. Gambhir SS, Mahoney DK, Huang SC, Phelps ME. Symbolic interactive modeling package and learning environment (SIMPLE): a new easy method for compartmental modeling. *Proc Soc Computer Simulation* 1996:173–186.
21. Heymann MA, Payne BD, Hoffman JIE, Rudolph AM. Blood flow measurements with radionuclide-labeled particles. *Prog Cardiovasc Dis* 1977;20:55–79.
22. Altman DG. *Practical statistics for medical research.* London: Chapman and Hall; 1991:189–191.
23. Lewis ML, Caterina RD, Giuntini C. Distribution function of transit times in the human pulmonary circulation. *J Appl Physiol* 1994;76:1363–1371.
24. Rosenspire K, Schwaiger M, Mangner T, Hutchins G, Sutorik A, Kuhl D. Metabolic fate of ^{13}N ammonia in human and canine blood. *J Nucl Med* 1990;31:163–167.
25. Mesterton-Gibbons MA. *Concrete approach to mathematical modeling.* Redwood City, CA: Addison-Wesley; 1989.

Direct Detection of Regional Myocardial Ischemia with Technetium-99m Nitroimidazole in Rabbits

Howard Weinstein, Christopher P. Reinhardt and Jeffrey A. Leppo

Departments of Nuclear Medicine and Medicine, Myocardial Isotope Research Lab, University of Massachusetts Medical Center, Worcester, Massachusetts

Conventional perfusion scintigraphy assesses disparities in regional myocardial blood flow but does not directly detect hypoxic tissue. Nitroimidazoles labeled with positron-emitting radionuclides have recently shown promise as direct markers of myocardial hypoxia. This study evaluates a new ^{99m}Tc-labeled nitroimidazole of potential benefit in standard myocardial scintigraphy. **Methods:** Technetium-99m-labeled nitroimidazole was administered to rabbits during the early reperfusion phase after 10 min (Group 1) or 60 (Group 2) min of coronary occlusion or after 10 min of a fixed coronary occlusion (Group 3). Tracer retention at 1 hr was assessed in relation to microsphere-determined blood flow during coronary occlusion and at tracer injection. The pattern of nitroimidazole retention on autoradiographs was then compared with the pattern of myocardial hypoperfusion defined by fluorescein photography to precisely define tracer localization. **Results:** The retention of nitroimidazole in Group 1 rabbits (brief occlusion) was independent of both occlusion and reperfusion blood flow and was uniformly distributed on the autoradiographs. In contrast, nitroimidazole retention in Groups 2 and 3 increased with the severity of hypoperfusion during the occlusion phase and precisely delineated the ischemic zone on all autoradiographs. **Conclusion:** This ^{99m}Tc-labeled hypoxia-avid tracer delineates severe ischemia even after blood flow to the compromised myocardium has been restored. This class of compounds can potentially enhance the physiological assessment of patients with ischemic heart disease.

Key Words: myocardial tracers; ischemia; technetium-99m nitroimidazole

J Nucl Med 1998; 39:598–607

Received Nov. 5, 1996; revision accepted Jul. 16, 1997.

For correspondence or reprints contact: Howard Weinstein, MD, University of Wisconsin, Milwaukee Clinical Campus, 960 N. 12th St., Milwaukee, WI 53233.

The presence of a stress-induced defect in regional myocardial perfusion on conventional scintigraphy with either ^{201}Tl or ^{99m}Tc-labeled agents has long been interpreted as evidence of ischemia. However, these radiopharmaceuticals only detect disparities in coronary blood flow and do not specifically localize hypoxic myocardium based on an imbalance between supply and demand. The development of "hot spot" imaging agents that directly concentrate in hypoxic tissue would enhance our ability to identify ischemic tissue.

Nitroimidazoles are hypoxia-avid compounds that localize and sensitize hypoxic neoplastic tissue before radiotherapy (*1–8*). If these agents localize selectively in hypoxic myocytes, they will have important clinical and experimental applications as direct markers of ischemia. Favorable results using nitroimidazoles labeled with positron-emitting radionuclides in basic cardiac studies (*9–12*) have fostered the development of such compounds labeled with single-photon emitters for conventional scintigraphy and basic experimental applications. Technetium-O-(PnAO-1-(2-nitroimidazole) (NI) (Fig. 1) (*13*), a new ^{99m}Tc-labeled nitroimidazole, was retained preferentially in hypoxic myocardium in preliminary studies (*14,15*).

Accordingly, we administered ^{99m}Tc-NI to 24 rabbits after brief or prolonged transient ischemic insults designed to produce regional myocardial hypoxia of graded severity and in the presence of a fixed coronary occlusion. We measured segmental ^{99m}Tc-NI uptake relative to absolute coronary blood flow and histochemically determined viability and, in a subgroup, compared the autoradiographic pattern of ^{99m}Tc-NI retention to the pattern of myocardial hypoperfusion.

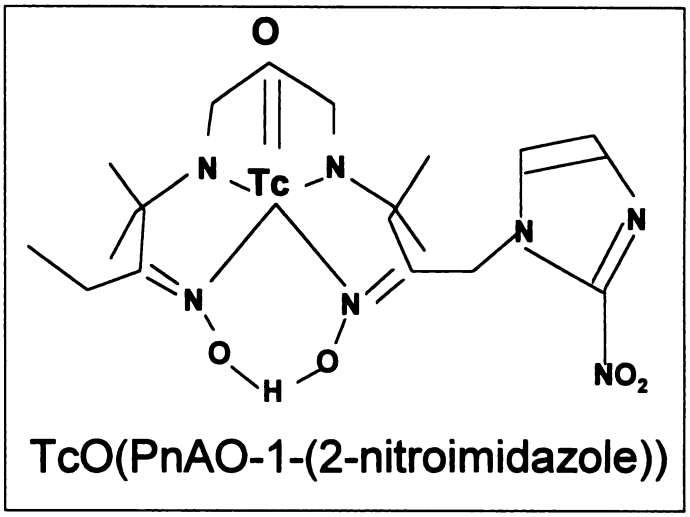

FIGURE 1. Chemical structure of ^{99m}Tc-NI.

MATERIALS AND METHODS

Preparation of Technetium-99m-NI

To each ^{99m}Tc-NI vial (Bristol-Myers Squibb Pharmaceutical, Princeton, NJ), 2 ml of $^{99m}TcO_4^-$ in saline were added, and the ligand was allowed to dissolve completely. In a separate vial, stannous DTPA (Squibb Techneplex) was reconstituted in 4 ml of saline, and 0.15 ml of the reconstituted Techneplex was added to the ligand. The solution was then allowed to stand at room temperature for 10 min. Radiochemical purity was verified by thin layer chromatography using Gelman solvent saturation pads spotted first with ethanol, then immediately with ^{99m}Tc-NI. Radiochemical purity was calculated as solvent front activity divided by total activity (solvent front + origin) × 100%. Radiochemical purity was confirmed to exceed 90% in all kits.

Surgical Procedure

Twenty-five New Zealand white rabbits (1.8–3.0 kg) were sedated with ketamine (35–50 mg/kg) and xylazine (5–10 mg/kg), intubated with a no. 2 or no. 3 pediatric endotracheal tube and artificially ventilated under 1%–2% nitrous oxide and 100% O_2 (Ohio 7000, Ohio Medical, Cleveland, OH). Vinyl catheters were inserted into a marginal ear vein, a carotid artery and both femoral arteries. A left lateral thoracotomy was performed in the fourth or fifth intercostal space, and the hearts were exposed in a pericardial cradle. The left atrium was then catheterized. The experimental subgroups are shown in Table 1.

Experimental Protocol

Group 1 (Brief Occlusion). The experimental design for the protocol using myocardial segmentation is shown in Figure 2. A large branch of the left circumflex coronary artery was isolated and occluded proximally for 10 min with a nondestructive vascular clamp. Severe hypoperfusion was visually confirmed by regional cyanosis and akinesia distal to the occlusion. At the end of the occlusion period, arterial blood was withdrawn for blood gas analysis. Radiolabeled microspheres (^{95}Nb, 12–15 μm, 5 × 10^5 spheres) were thoroughly agitated and injected into the left atrium, and a reference blood sample was simultaneously withdrawn from the femoral artery to assess regional blood flow during coronary occlusion. The clamp was then released, and reperfusion was noted visually by the restoration of normal myocardial color and activity. Three minutes after release of the occluder, a second set of radiolabeled microspheres (^{51}Cr) was then injected into the left atrium, and blood was simultaneously withdrawn from the femoral artery to define reperfusion blood flow. Thirty microcuries of ^{99m}Tc-NI was then injected intravenously and allowed to circulate for 60 min. Blood samples were obtained from the second femoral artery catheter 30 sec and 1 min after ^{99m}Tc-NI injection, every minute for 10 min, then every 5 min until death. The brief occlusion (Group 1) was designed to simulate the transient ischemic episodes occurring in ischemia at rest or after exercise or pharmacological stress.

Group 2 (Prolonged Occlusion). To evaluate ^{99m}Tc-NI retention in the presence of significant infarction, we sustained coronary occlusion for 60 min in the rabbits in Group 2, sufficient to produce substantial transmural myocardial necrosis (*16–18*). The protocol was otherwise identical to that of Group 1, with the tracer once again injected 3 min after release of the occluder. This intervention was designed to simulate prolonged ischemia followed by the restoration of blood flow, as occurs in an acute myocardial infarction with spontaneous or induced reperfusion.

Group 3 (Fixed Occlusion). To evaluate ^{99m}Tc-NI uptake in a model of fixed coronary occlusion, we subjected rabbits in Group 3 to coronary occlusion for 10 min with no reperfusion. After 10 min of occlusion, ^{99m}Tc-NI was injected intravenously and was allowed to circulate for 1 hr during which the occlusion was sustained. Thus, the tracer was injected and allowed to interact with ischemic myocytes in the presence of severe myocardial ischemia but before substantial transmural infarction was likely to have occurred (*16*). Radiolabeled microspheres (^{95}Nb) were injected in the basal state and after coronary occlusion (^{103}Ru). The protocol then proceeded as in Group 1. The fixed occlusion was designed to simulate severe acute ischemia without reperfusion.

This experimental model of complete coronary occlusion produces graded ischemia within each rabbit (*19*). Therefore, among the three experimental protocols, a wide range of myocardial ischemia and cellular viability was produced, reflecting the diversity of ischemic clinical syndromes.

TABLE 1
Experimental Subgroups

	Group 1	Group 2	Group 3	Control	Total
Time of ischemia	10 min	60 min	10 min	–	
Time of reperfusion	3 min	3 min	–	–	
Segmental analysis (n)	6	6	4	0	16
Autoradiography (n)	2	2	2	2	8
Total					24

Tissue Processing

At the end of the circulation period, cardiac asystole was induced by an intra-atrial injection of KCl, and the hearts were excised. The atria and right ventricles were removed, and the hearts were frozen at 0°C for 30 min. Approximately 60 transmural left ventricular segments were then weighed, placed in test tubes and assessed for myocardial viability as described later.

Determination of Myocardial Viability

Myocardial viability was assessed, uniformly for the three groups, by standard histochemical staining techniques with tetrazolium salts (*20–22*), as previously used in similar rabbits models (*16*). For each experiment, 0.75 ml of a 0.5 mg% solution of the vital stain nitro-blue tetrazolium (NBT) in phosphate buffer (pH 8.0) was added to each myocardial segment and was incubated for 10 min at 37°C. Myocardial segments were then independently assessed for staining. Segmental viability was defined subjectively by the presence of greater than 75% blue staining, whereas infarct was inferred when less than 25% of the segment was stained. Segments with intermediate staining were designated as mosaic (partially infarcted). The entire contents of the NBT bath were then counted for microspheres and ^{99m}Tc to account for any activity extracted from the myocardium by the histochemical stain (*23*).

Determination of Segmental Tracer Activity

Tracer activity was determined in a gamma well-counter for 2 min (one determination per specimen), using triple energy windows for ^{99m}Tc-NI (^{99m}Tc, 130 ± 20 keV) occlusion flow (^{95}Nb, 725 ± 25 keV) and reperfusion flow (^{51}Cr, 320 ± 40 keV or ^{103}Ru, 503 ± 18 keV). All samples were corrected for inter-radionuclide crossover and radionuclide decay. Absolute myocardial blood flow by radiolabeled microsphere injection (*24*) was determined by the method of Heymann et al. (*25*), as applied previously in the rabbit model (*26*). In brief, blood flow in each myocardial segment is determined by the following equation:

$$\text{Myocardial blood flow (ml/min/g)} = \text{blood flow in reference arterial sample (ml/min)} \times \text{microsphere content of myocardial segment/microsphere content of reference arterial sample} \times \text{weight of myocardial segment (g).} \quad \text{Eq. 1}$$

Data Analysis

For each heart, relative segmental ^{99m}Tc activity (defined as segmental activity/segmental weight divided by total left ventricular activity/total left ventricular weight) was plotted against absolute segmental myocardial blood flow. Then, for each of the three intervention groups, segments were subdivided by absolute myocardial blood flow during occlusion, and the mean relative segmental ^{99m}Tc-NI activity was determined for each level of blood flow. For rabbits in Group 2 (prolonged occlusion), segments from each histochemical staining category were then considered separately to determine the influence of cellular viability on ^{99m}Tc-NI retention.

Determination of Blood Technetium-99m Activity

For each rabbit, blood ^{99m}Tc activity was determined by gamma well counting and fitted to a triexponential function. Percent of injected dose retained in the heart was calculated as the total left ventricular activity divided by the total injected activity (corrected for decay) × 100%.

Autoradiography and Fluorescein Photography

To precisely localize ^{99m}Tc-NI uptake in relation to regional myocardial hypoperfusion, the experimental protocol described previously was adapted for autoradiography. Rabbits (n = 2 per group) received a coronary occlusion followed by reperfusion (Groups 1 and 2) or a fixed coronary occlusion (Group 3), followed by ^{99m}Tc-NI injection. Microspheres were not administered. Instead, at the end of the ^{99m}Tc-NI circulation period, the arteries were reoccluded (Groups 1 and 2) and 80-mg sodium fluorescein was injected intravenously (all groups) to define the area of

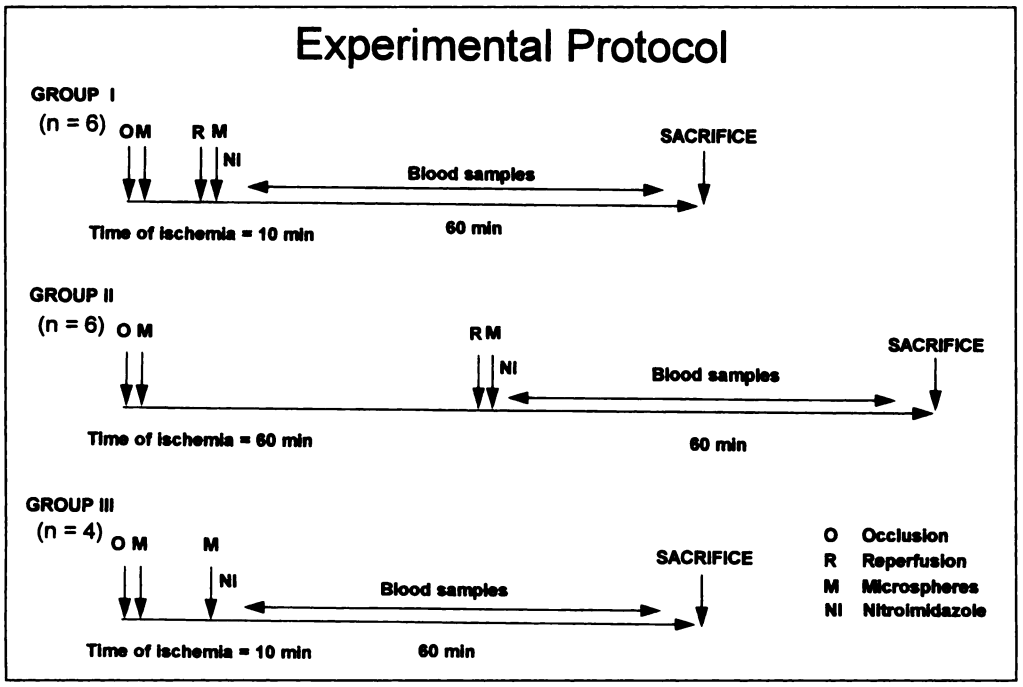

FIGURE 2. Experimental protocol. Autoradiography studies are not shown.

TABLE 2
Area at Risk

Rabbit	Group 1			Group 2			Group 3		
	AAR	NZ	Risk ratio	AAR	NZ	Risk ratio	AAR	NZ	Risk ratio
R1	1712	2646	0.393*	710	2005	0.262	617	2169	0.221
R2	1649	2254	0.422	1490	1501	0.498	274	2360	0.104
R3	857	2653	0.244	1237	1657	0.427	436	1939	0.184
R4	453	3293	0.121	845	2318	0.267	591	1828	0.244
R5	574	3592	0.138	871	2018	0.301			
R6	1349	2935	0.315	300	2274	0.117			
Mean	1099	2896	0.272	909	1962	0.312	480	2074	0.188
s.d.	546	485	0.127	515	327	0.135	159	238	0.062

*p = ns for risk ratio between Groups 1, 2 and 3.

AAR = area at risk, defined as the left ventricular mass (mg) with <0.50 ml/g/min blood flow during coronary occlusion; NZ = normal zone, defined as the left ventricular mass (mg) with >0.50 ml/g/min blood flow during coronary occlusion; Risk ratio = area at risk divided by total left ventricular mass.

hypoperfusion. The hearts were then excised and washed; the ventricles were filled with embedding medium (O.C.T., Miles, Inc., Elkhart, IN) and were quick-frozen in liquid nitrogen.

Multiple 30 μm short-axis slices from each heart were collected on tape (Type 820, 3M, St. Paul, MN) in a cryomicrotome (PMV 2250, LKB Instruments, Gaithersburg, MD), air-dried at room temperature and mounted face-up on cardboard. The heart slices were then placed on single-coated radiograph film (MRM-1, Eastman Kodak, Rochester, NY), vacuum sealed in black plastic bags to ensure direct apposition to the film and set aside for 18–24 hr to produce ^{99m}Tc autoradiographs. Films were then developed in an automatic radiograph film processor (RP X-OMAT, Eastman Kodak, Rochester, NY). The heart slices were then photographed under ultraviolet light to record the distribution of fluorescein, representing myocardial perfusion during coronary occlusion.

Control Measurements

Two sham-operated rabbits were injected with ^{99m}Tc-NI and processed for autoradiography to exclude focal retention of the tracer resulting from the surgical technique. No focal ^{99m}Tc-NI retention was noted on any autoradiographic heart slice from this control group.

Statistical Methods

Comparisons of ^{99m}Tc-NI retention between blood flow subgroups were made by analysis of variance (ANOVA). Comparisons between viable, mosaic and infarct groups were made using the Kruksal-Wallis one-way ANOVA on rank and Dunn's multiple comparison test (for nonparametric data).

RESULTS

Surgical Intervention

For all experimental protocols, arterial blood gas parameters remained physiologic (pH = 7.35–7.45; pCO_2 = 30–40 mm Hg; arterial pO_2 > 100 mm Hg). There was no difference between the three intervention groups in the area-at-risk ratio, defined as the proportion of left ventricular mass with blood flow < 0.50 ml/min/g (Table 2). Vital staining was normal in all segments from rabbits in Group 1 (brief occlusion), indicating preserved myocardial viability. In Group 3 (fixed occlusion), histochemical staining was normal but may have underestimated infarction due to insufficient washout of cellular dehydrogenases (*20*). Although myocardial infarction determined at the end of the experiment may have been underestimated, this intervention would not have been expected to produce infarction at the time of tracer injection (*16*).

Influence of Blood Flow on Technetium-99m-NI Retention

Group 1 (Brief Occlusion). Retention of ^{99m}Tc-NI was independent of blood flow measured either during occlusion (Fig. 3; Group 1) or at tracer injection during reperfusion. Data from a representative rabbit is shown in Figure 4, demonstrating no correlation between ^{99m}Tc-NI retention at 1 hr and either blood flow during reperfusion or during occlusion. On release of the occluder, substantial reperfusion was achieved (Fig. 4A).

Groups 2 (Prolonged Occlusion) and 3 (Fixed Occlusion). In contrast to Group 1, relative ^{99m}Tc-NI activity increased with decreasing occlusion blood flow in both Groups 2 and 3 (Fig. 3). Individual plots of ^{99m}Tc-NI retention versus absolute coronary blood flow during occlusion are shown for the six rabbits in Group 2 (Fig. 5) and the four rabbits in Group 3 (Fig. 6). In Group 2, retention of ^{99m}Tc-NI increased sharply in each heart when blood flow during coronary occlusion fell below an inflection point of approximately 0.4 ml/min/g. In Group 3 (fixed occlusion), the data were less well ordered, with a tendency to highly variable ^{99m}Tc-NI values at the lower limits of occlusion blood flow (Figs. 3 and 6), reflecting impaired delivery of the tracer to the hypoperfused zones. In both groups, ^{99m}Tc-NI retention was again independent of blood flow at the time of tracer injection (not shown).

Influence of Myocardial Viability on Technetium-99m-NI Retention

Segments from Group 2 (the only group with detectable infarction) were then subdivided by histochemical staining to determine if ^{99m}Tc-NI retention is influenced by cellular viability (Fig. 7). As expected, segments showing predominant or partial (mosaic) infarction by histochemical staining received significantly reduced blood flow during coronary occlusion compared to viable segments. Substantial reperfusion was achieved in all subgroups. Despite similar blood flows at tracer injection, segments with predominant or partial infarction (mosaic) showed increased ^{99m}Tc-NI retention at 1 hr as compared to segments with normal vital staining.

Autoradiography/Fluorescein Photography

Group 1 (Brief Occlusion). All heart slices showed faint, homogeneous ^{99m}Tc activity despite large defects in fluorescein uptake indicating severe hypoperfusion during the period of coronary occlusion.

Group 2 (Prolonged Occlusion). On all heart slices, there was focal transmural ^{99m}Tc activity that corresponded closely with the area of hypoperfusion (Fig. 8).

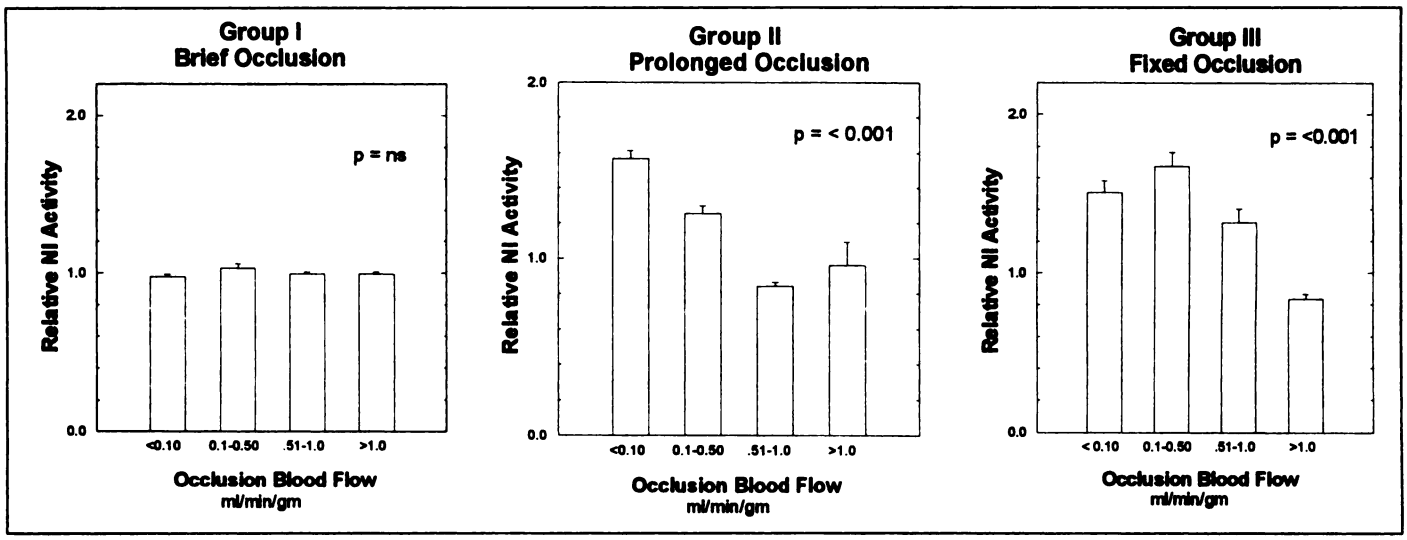

FIGURE 3. Influence of absolute myocardial blood flow during coronary occlusion on segmental ^{99m}Tc-NI retention in the three groups. Error bars represent 1 s.e.m. Retention of ^{99m}Tc-NI increased in Groups 2 and 3 as hypoperfusion during the occlusion phase became more severe. Where tracer delivery was restricted (fixed occlusion), ^{99m}Tc-NI activity decreased at the lower limit of blood flow measurement. Retention of ^{99m}Tc-NI after a brief occlusion (Group 1) was independent of blood flow during the occlusion phase.

Group 3 (Fixed Occlusion). As in Group 2, focal ^{99m}Tc activity was observed that overlapped the areas of hypoperfusion. The ischemic zone was not reperfused in this group, and the resulting pattern of ^{99m}Tc-NI activity was restricted to the periphery of the fluorescein defects represented by the dark areas (Fig. 9).

Blood Kinetics

Blood ^{99m}Tc activity was triphasic, with a rapid decline followed by a prolonged plateau (Fig. 10). The mean residual blood activity at 60 min was 0.22, 0.32 and 0.34 of the activity measured 30 sec postinjection for Groups 1, 2 and 3 rabbits, respectively (Table 3). Median half-times for blood clearance were 0.405 min ($T_{½1}$), 2.42 min ($T_{½2}$) and 1368 min ($T_{½3}$). Total myocardial ^{99m}Tc-NI retention as a proportion of the injected ^{99m}Tc activity was 0.10% ± 0.02%.

DISCUSSION

Nitroimidazoles and other heterocyclic amines are metabolically active agents that integrate into endogenous cellular electron transfer pathways (*7,27,28*). They are metabolized to radical intermediates by cellular reductases and, under hypoxic conditions, undergo further metabolism to a variety of nitroso compounds, hydroxylamines and amines. These reduction products of anaerobic metabolism react covalently with cellular macromolecules and are trapped. The metabolism of the nitroimidazoles has been extensively studied (*2,7,27–30*).

Localization in Ischemic Regions

In this study, ^{99m}Tc-NI retention 1 hr after tracer injection increased selectively in both ischemic and postischemic myocardium. Because supplemental oxygen was administered to all rabbits to prevent hypoxemia, this selective retention of the tracer in hypoperfused myocardium represents a direct response to local metabolic conditions. Moreover, the retention of ^{99m}Tc-NI directly correlated with the degree of regional hypoperfusion produced in Groups 2 (prolonged occlusion) and 3 (fixed occlusion) rabbits. The localization of ^{99m}Tc-NI in ischemic tissue was confirmed by autoradiographs showing concordant areas of ^{99m}Tc-NI retention and hypoperfusion (as defined by fluorescein defects). When tracer delivery to the central ischemic areas was restricted (Group 3; fixed occlusion), ^{99m}Tc-NI retention was limited to the border areas around the zone of hypoperfusion, reflecting collateral flow (*31*).

It is important to define both the degree of ischemia that can be identified by hypoxia markers and the optimal time to administer these compounds in relation to an ischemic insult. In

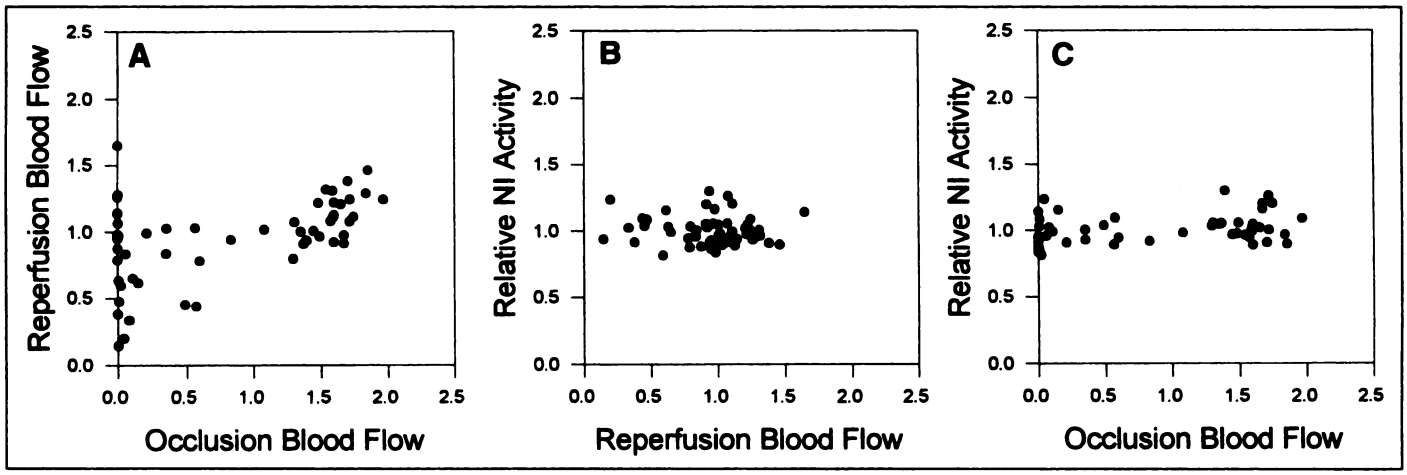

FIGURE 4. Data from a rabbit in Group 1 (brief occlusion). Myocardial perfusion was substantially restored after coronary occlusion (A). Retention of ^{99m}Tc-NI at 1 hr was independent of blood flow during both reperfusion (B) and occlusion (C).

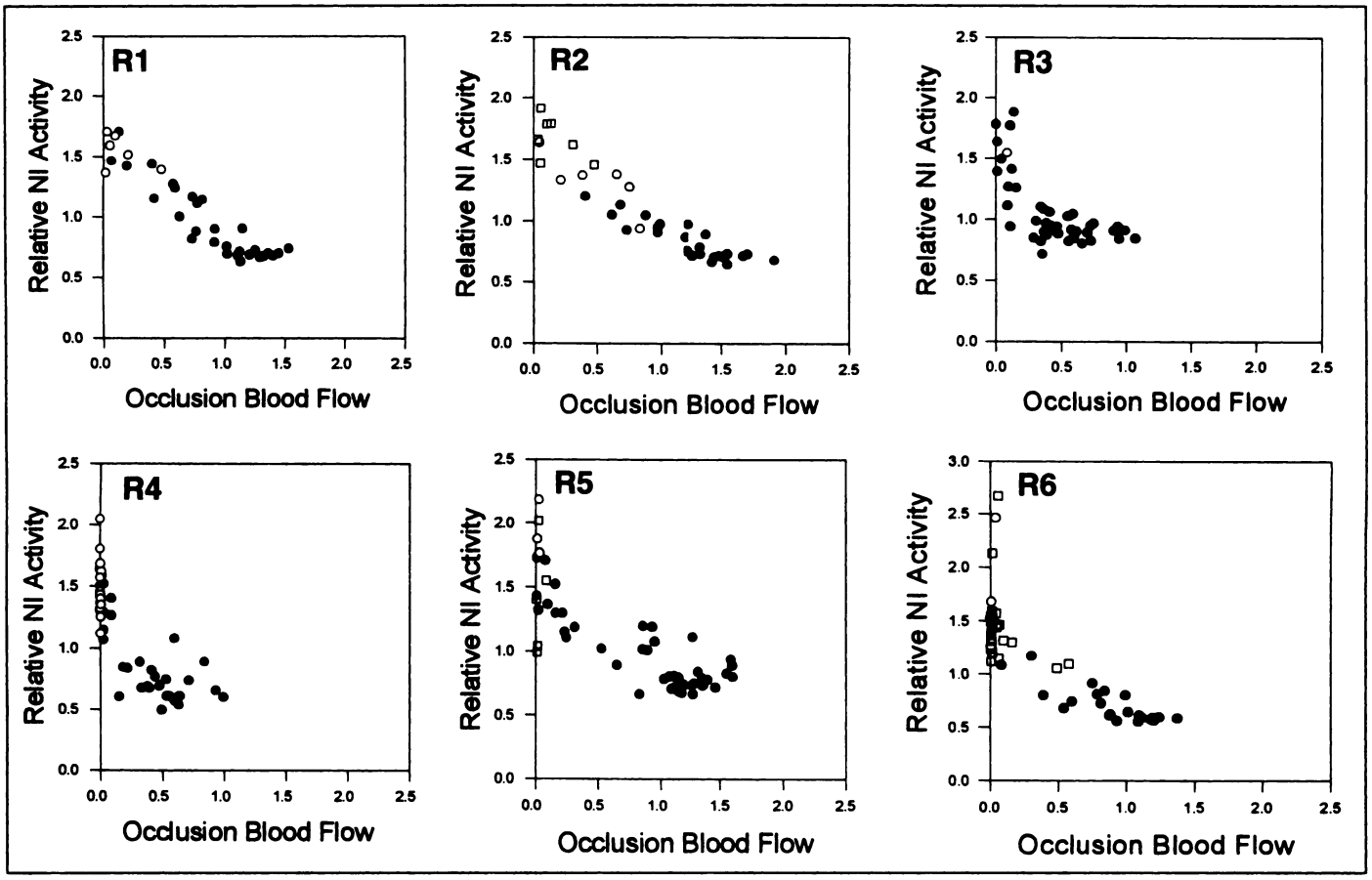

FIGURE 5. Influence of absolute myocardial blood flow (ml/min/g) during coronary occlusion on segmental ^{99m}Tc-NI retention in individual rabbits in Group 2 (prolonged occlusion). Solid circles represent viable segments, and hollow circles and squares represent partially infarcted and infarcted segments. Retention of ^{99m}Tc-NI increased as hypoperfusion during the occlusion phase became more severe.

this study, ^{99m}Tc-NI was selectively retained (at 1 hr) when injected in the presence of low-flow ischemia but before substantial transmural infarction was likely to have occurred (*16*) (evidenced by normal NBT histochemical staining; Group 3) or after a 1-hr episode of severe ischemia (Group 2). In contrast, no selective regional ^{99m}Tc-NI activity was noted after a brief ischemic insult that did not produce infarction (Group 1). Hence, if the ischemia is relatively brief, minimal reperfusion may be sufficient to raise local tissue oxygen concentration beyond the critical threshold for ^{99m}Tc-NI retention. Selective myocardial retention of this ^{99m}Tc-labeled nitroimidazole, therefore, requires severe ischemia without sufficient time for recovery.

A similar relation between tracer retention and ischemia was demonstrated as well for ^{18}F-fluoromisonidazole by Shelton et al. (*10*) in the isolated perfused rabbit heart. In that study, ^{18}F-fluoromisonidazole retention was increased by both low-flow ischemia and normal-flow hypoxemia but not by 35 min of ischemia followed by 20 min of reperfusion. Their findings provide evidence that myocardial nitroimidazole retention is directly related to cellular hypoxia. As demonstrated by Martin et al. (*32*) in the intact canine heart, nitroimidazole retention reflects the regional delivery of oxygen *relative to demand*. They observed focal nitroimidazole retention after hyperemic regional coronary blood flow in the distribution of a partially occluded coronary artery when demand was increased by the combined effects of catecholamine administration and cardiac pacing. They further noted enhanced nitroimidazole retention in the subendocardium despite increased blood flow in that region during the ischemic period. Hence, nitroimidazoles can identify

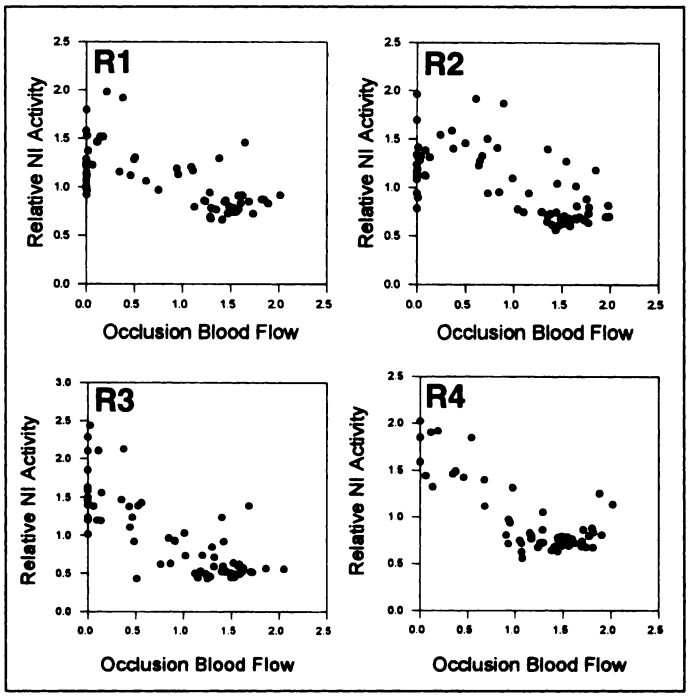

FIGURE 6. Influence of absolute myocardial blood flow (ml/min/g) during coronary occlusion on segmental ^{99m}Tc-NI retention in individual rabbits in Group 3 (fixed occlusion). Retention of ^{99m}Tc-NI increased as hypoperfusion during the occlusion phase became more severe. Where tracer delivery was restricted in this nonreperfused group, ^{99m}Tc-NI activity varied significantly at the lower limit of blood flow measurement.

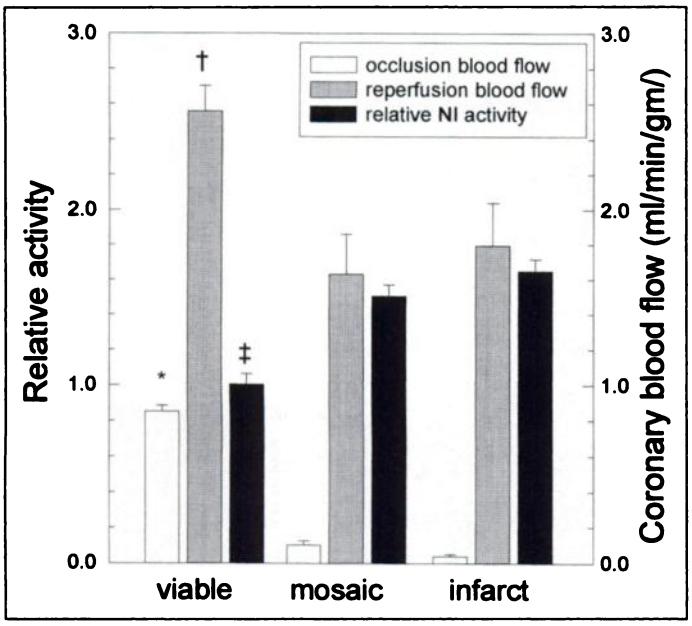

FIGURE 7. Influence of myocardial viability on ^{99m}Tc-NI retention in rabbits from Group 2 (prolonged occlusion). Mean relative tracer retention is plotted for segments defined by histochemical staining as viable, mosaic and infarcted. Mean absolute occlusion and absolute reperfusion blood flows are also shown. Retention of ^{99m}Tc-NI was significantly increased, and blood flow during coronary occlusion was reduced, in infarcted and partially infarcted (mosaic) segments, compared with viable segments. *$p < 0.05$ for viable versus mosaic and viable versus infarcted. †$p < 0.05$ for viable versus mosaic only. ‡$p < 0.05$ for viable versus infarct and viable versus infarct.

ischemic metabolism in the absence of reduced coronary blood flow if blood flow is inadequate to meet local oxygen requirements.

Relationship of Technetium-99m-NI to Regional Blood Flow

Retention of ^{99m}Tc-NI increased steeply when local blood flow decreased below the inflection point (Figs. 5 and 6). The increase in relative ^{99m}Tc-NI retention at approximately 0.4 ml/min/g of blood flow in rabbits in Groups 2 and 3 agrees closely with previous studies on nitroimidazoles (*9,11,32,33*). Moreover, in the isolated perfused heart (*12*), nitroimidazole retention was greater in anoxic than in hypoxic tissue. Hence, this class of compounds can differentiate gradations in local hypoxia.

Myocardial ^{99m}Tc-NI retention correlated closely with local blood flow during the occlusion period (in Groups 2 and 3) but was independent of the perfusion pattern at the time of tracer injection. This selective retention of ^{99m}Tc-NI in reperfused postischemic tissue represents a "memory effect" in that the myocardial distribution of ^{99m}Tc-NI measured 1 hr after injection is predetermined by the earlier ischemic insult and not by the perfusion status at tracer injection. Although the retention of nitroimidazoles depends ultimately on the extent of the ischemic insult, minimal blood flow is required to deliver the tracer to hypoxic tissue (Fig. 9), as noted previously (*11*).

Dependence on Cellular Viability

The ability of nitroimidazoles to identify acutely or chronically ischemic myocardium (jeopardized or hibernating) and to direct coronary revascularization would be limited if their relationship to cellular viability was unpredictable. The retention of nitroimidazoles, in theory, requires intact cellular reductases, hence myocardial viability (*2,7,27–29*). The results of this study and others, however, suggest that *acutely* injured hypoxic myocytes that are no longer viable can, at least initially, retain nitroimidazoles. Previous work using postmortem histochemical or pathologic analysis has likewise shown that the nitroimidazoles are selectively retained in acutely necrotic tissue. Martin et al. (*33*), using a positron-emitting nitroimidazole in dogs, showed tracer accumulation in both viable and nonviable ischemic segments 4 hr after complete occlusion of the left anterior descending coronary artery. In a separate study of the same compound (*11*), these investigators again demonstrated nitroimidazole retention in acutely necrotic myocardium distal to a coronary occlusion. The ability of acutely necrotic, hypoxic myocytes to retain nitroimidazoles diminishes, however, with time from the acute insult. Shelton et al. (*9*) showed a progressive decrease in fluoromisonidazole

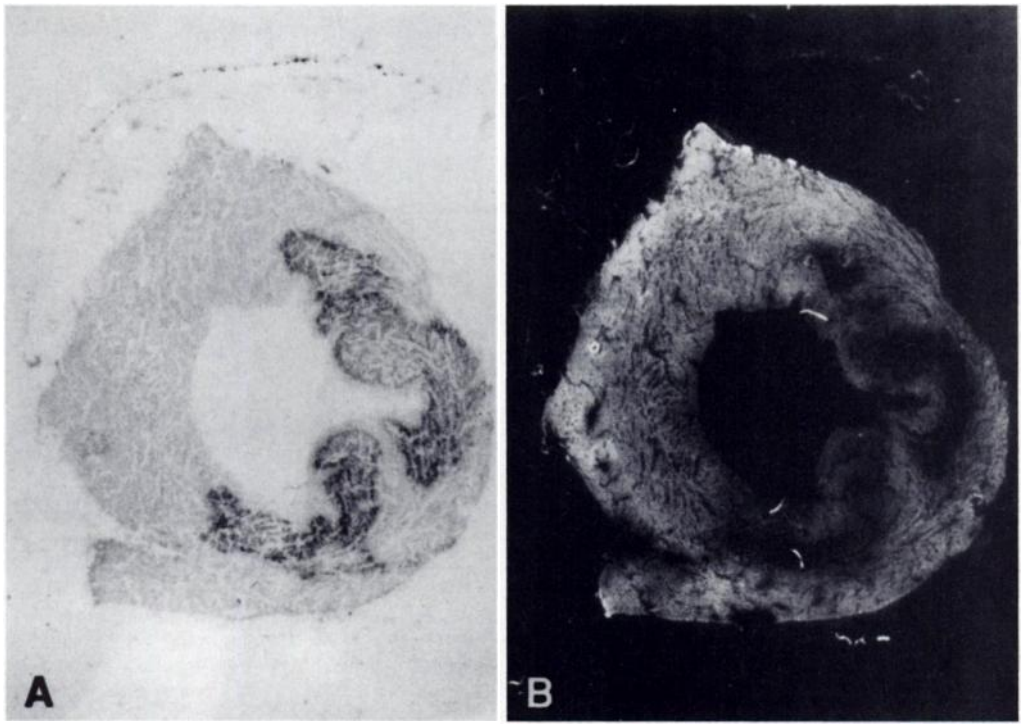

FIGURE 8. Autoradiograph of ^{99m}Tc-NI retention (A) and corresponding fluorescein photograph (B) of a 30-μm heart slice from a rabbit in Group 2 (prolonged occlusion). The area of focal ^{99m}Tc-NI retention corresponds closely with the area of reduced fluorescein uptake (intramyocardial dark area) that delineated myocardial hypoperfusion during the occlusion phase. A partial rim of increased ^{99m}Tc-NI activity is visible at the outer margin of the hypoperfused zone.

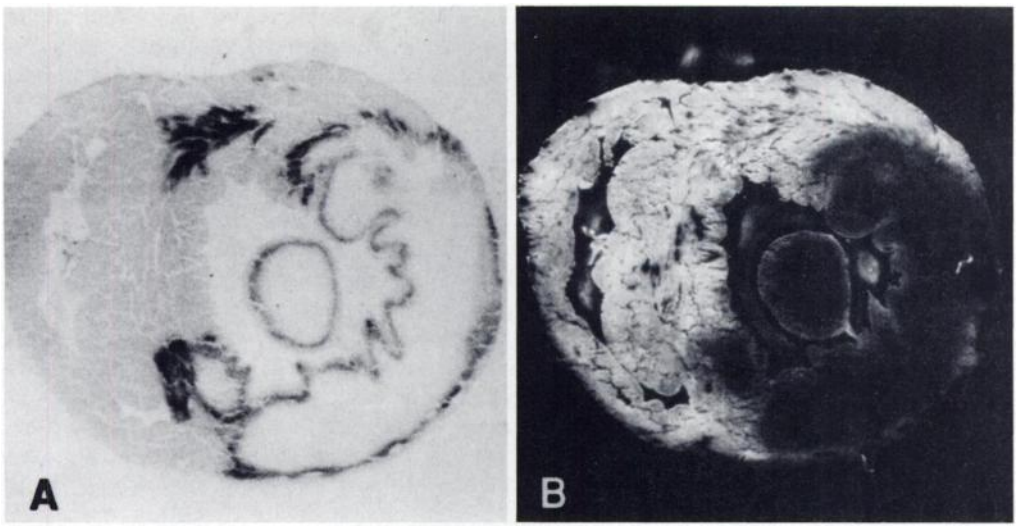

FIGURE 9. Autoradiograph of ^{99m}Tc-NI retention (A) and corresponding fluorescein photograph (B) of a 30-μm heart slice from a rabbit in Group 3 (fixed occlusion). A rim of focal ^{99m}Tc-NI activity is seen at the perimeter of the zone of hypoperfusion (dark area on fluorescein image) in this nonreperfused rabbit.

activity in the ischemic regions of dogs subjected to 3, 6 or 24 hr of complete coronary occlusion. Thus, nitroimidazoles may be retained in acutely necrotic hypoxic tissue until specific reductases are washed out or until the plasma membrane is disrupted or a combination of both.

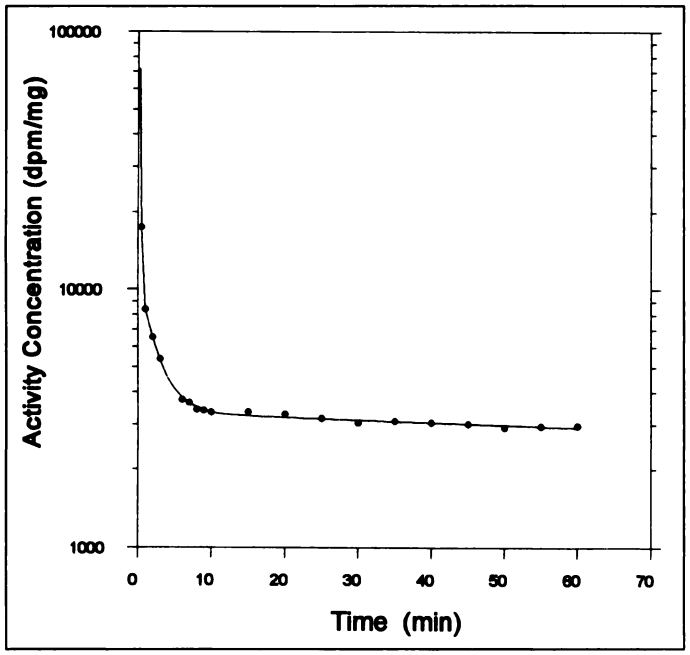

FIGURE 10. Blood kinetics of ^{99m}Tc-NI in one rabbit.

TABLE 3
Blood Kinetics

Rabbit	Group 1*	Group 2	Group 3
R1	0.275	0.170	0.319
R2	0.183	0.534	0.404
R3	0.246	0.342	0.350
R4	0.192	0.370	0.286
R5	0.410	0.287	
R6	0.026	0.187	
Mean	0.222	0.315	0.340
s.d.	0.126	0.134	0.050

*p = ns between Groups 1, 2 and 3 by analysis of variance.

Residual blood ^{99m}Tc activity at 60 min postinjection as a proportion of initial activity.

The relationship between ^{99m}Tc-NI retention and myocardial viability may also be influenced by the radiolabel. As pointed out in the Study Limitations section, the binding of the nitroimidazoles to hypoxic myocardial tissue may involve molecular fragments rather than the parent compounds (*7*). Thus, the retention of the ^{99m}Tc-labeled nitroimidazoles in acutely infarcted tissue may result from the specific binding properties of the ^{99m}Tc-^{99m}Tc-NI complex.

Technetium-99m-NI Retention: Percent of Injected Activity and Regional Activity Contrast

Total myocardial ^{99m}Tc-NI retention as a proportion of the injected ^{99m}Tc activity was 0.10% ± 0.02%, consistent with values obtained for fluoromisonidazole in dogs (*11*). Although the global retention of a myocardial tracer is important in clinical scintigraphy, it is more important that specifically directed tracers (such as hypoxia probes) exhibit adequate target-to-background contrast. Indeed, fluoromisonidazole showed higher relative regional myocardial activity in acutely ischemic, nonviable tissue than contemporaneously injected ^{99m}Tc-pyrophosphate (*33*) (a clinically validated infarct-avid tracer). Tissue-to-blood-pool activity increases with time after nitroimidazole injection (*33*); thus, myocardial ^{99m}Tc-NI activity and regional ^{99m}Tc-NI target-to-background contrast may be optimized in subsequent protocols.

Ischemic-to-normal myocardial ^{99m}Tc-NI retention was approximately 1.5–3.5 in this study, as determined by segmental analysis. These values are consistent with data obtained by Martin et al. (*32*) (iodovinylmisonidazole) in the intact canine heart and by Shelton et al. (*10*) (fluoromisonidazole) in the isolated perfused rabbit heart. The activity contrast between ischemic and normal myocardium exhibited by the nitroimidazoles is similar to other specifically targeted radiotracers as well, such as ^{99m}Tc-pyrophosphate (*33*) and ^{111}In-antimyosin antibodies (contrast to normal myocardium of 4:1 and 3:1 for infarcted and for partially infarcted tissue, respectively) (*34*). Thus, based on this study and on previous work on positron-emitting nitroimidazoles, this class of compounds can potentially exhibit sufficient contrast for both diagnostic imaging and basic cardiac research.

Although we did not evaluate hepatic ^{99m}Tc-NI retention, previous studies suggest interference from hepatic ^{99m}Tc-NI activity as a potential problem in clinical imaging with these compounds. Shi et al. (*35*) demonstrated increasing hepatic activity over time after ^{99m}Tc-misonidazole injection in dogs, with a liver:heart ratio of 4.2 at 60 min after injection,

somewhat higher than the analogous values of ~2–2.5 at 4 hr postinjection derived from tritiated nitroimidazoles (*11,36*).

Blood Kinetics

Blood ^{99m}Tc-NI levels declined rapidly after tracer injection, reaching a plateau at a variable fraction of the initial blood level (Table 3). When fitted to a triexponential function to precisely define blood ^{99m}Tc-NI decay (*37*), the median $t_{1/2}$ values were 0.405 min, 2.42 min and 1368 min for the early, intermediate and late decay, respectively. Both the blood decay pattern and the fractional residual blood ^{99m}Tc-NI activity at plateau agree with the decay of scintigraphic left atrial (*9*) and left ventricular (*33*) ^{18}F-fluoromisonidazole and of arterial ^{131}I-iodovinylmisonidazole (*32*) activity.

Based on the present pharmacokinetic data and on data from previous studies (*9,32,33*), we conclude that the residual blood pool ^{99m}Tc-NI activity may complicate but would not by itself preclude external gamma camera imaging. In previous studies (*11,36*), tracer activity in the blood pool did not exceed ^{99m}Tc-NI activity in normal myocardial tissue. Thus, as demonstrated experimentally, enhanced ^{99m}Tc-NI retention in ischemic or postischemic tissue should be discernable by both conventional scintigraphy (*35*) and by PET (*9*) under appropriate imaging conditions.

Study Limitations

The segmental and autoradiographic analyses used in this study are inherently limited to a single determination of myocardial tracer distribution for each specimen. The relationship observed between occlusion blood flow and ^{99m}Tc-NI activity was likely influenced by the interval between tracer injection and death. Both the accumulation of nitroimidazoles in cultured cells (*12*) and the activity contrast between ischemic and normal myocardium (*33*) continue to increase with time after administration of the tracer. The clinically practical interval between injection and imaging, however, is limited by the brief half-life of the ^{99m}Tc label (6 hr) and by scheduling considerations. Hence, a circulation time of 1 hr was selected in this study, in keeping with earlier, preliminary work on this compound (*14*).

As mentioned earlier, the experimental protocol may have precluded the detection of infarction by histochemical staining in Group 3 rabbits (despite an overall duration of ischemia of 70 min) by preventing the release of dehydrogenases from these nonreperfused hearts. However, at the time the tracer was injected and reacted with ischemic myocytes (10 min of coronary occlusion), significant infarction was unlikely to have occurred. Our protocol was confined to acute ischemia and infarction. Therefore, further studies in subacute and chronic models of ischemia and infarction are warranted.

This study relates ^{99m}Tc-NI activity to regional myocardial blood flow during coronary occlusion (all groups) and reperfusion (Groups 1 and 2), but it does not directly measure local tissue hypoxia. It is conceivable, therefore, that ^{99m}Tc-NI retention was induced not by hypoxia per se but by the presence (or absence) of an as yet unknown metabolic factor associated with myocardial ischemia. The dependence of nitroimidazole retention on cellular hypoxia has been established in basic oncologic tissue and cell culture, in myocytes (*12*) and in the isolated perfused heart (*10*) and was therefore not defined further in this study.

This class of compounds differentiates hypoxic myocytes from the surrounding myocardial tissue. The nature and location of the radiolabel is important in the biodistribution and kinetics of many radiotracers, and chelation with metals such as technetium has historically proven problematic in preserving the bioactivity of the parent compound (*38*). The effect of the radiolabel is particularly germane with nitroimidazoles because their tissue binding may occur through molecular fragments (*7*). Thus, the location and stability of the radiolabel is critical to the efficacy of hypoxia markers and may account for the specific properties of the individual compounds.

CONCLUSION

This study demonstrates the potential application of hypoxia markers to single photon scintigraphy because of their ability to concentrate selectively in myocardial regions hypoperfused *before but not necessarily at the time of* tracer injection. Although the imaging capabilities of this ^{99m}Tc-labeled compound are uncertain, the ability of the nitroimidazoles to localize in recently or actively ischemic myocardium has important implications in the assessment of patients with ischemic heart disease. Moreover, as demonstrated by previous studies, this class of compounds can directly identify inadequate perfusion in relation to demand. Such a direct functional assessment of the adequacy of myocardial perfusion would be unique among single photon tracers and warrants further investigation to develop this potential.

ACKNOWLEDGMENTS

This manuscript was supported in part by National Institutes of Health Research grant RO1 HL 34199 and by Bristol-Myers Squibb Pharmaceutical. We thank Robin Marcel for expert technical support and Harriet Kay and Pam Lynde for secretarial assistance.

REFERENCES

1. Miller GG, Ngan-Lee J, Chapman JD. Intracellular localization of radioactively labelled misonidazole in EMT-6 tumor cells in vitro. *Int J Radiatology Oncology Biol Phys* 1982;8:741–744.
2. Adams GE, Stratford IJ. Hypoxia-mediated nitro-heterocyclic drugs in the radio- and chemotherapy of cancer: an overview. *Biochem Pharmacol* 1986;35:71–76.
3. Chapman JD. Current concepts in cancer: hypoxic sensitizers—implications for radiation therapy. *N Engl J Med* 1979;301:1429–1432.
4. Rasey JS, Grunbaum Z, Magee S, et al. Characterization of radiolabeled fluoromisonidazole as a probe for hypoxic cells. *Rad Res* 1987;111:292–304.
5. Rasey JS, Koh W-J, Grierson JR, Grunbaum Z, Krohn KA. Radiolabeled fluoromisonidazole as an imaging agent for tumor hypoxia. *Intl J Radiat Oncol Biol Phys* 1989;17:985–991.
6. Chapman JD, Franko AJ, Sharplin J. A marker for hypoxic cells in tumours with potential clinical applicability. *Br J Cancer* 1981;43:546–550.
7. Franko AJ. Misonidazole and other hypoxia markers: metabolism and applications. *Intl J Radiat Oncol Biol Phys* 1986;12:1195–1202.
8. Valk PE, Mathis CA, Prados MD, Gilbert JC, Budinger TF. Hypoxia in human gliomas: demonstration by PET with fluorine-18-fluoromisonidazole. *J Nucl Med* 1992;33:2133–2137.
9. Shelton ME, Dence CS, Hwang D-R, Herrero P, Welch MJ, Bergmann SR. In vivo delineation of myocardial hypoxia during coronary occlusion using fluorine-18-fluoromisonidazole and positron emission tomography: a potential approach for identification of jeopardized myocardium. *J Am Coll Cardiol* 1990;16:477–485.
10. Shelton ME, Dence CS, Hwang D-R, Welch MJ, Bergmann SR. Myocardial kinetics of fluorine-18 misonidazole: a marker of hypoxic myocardium. *J Nucl Med* 1989;30:351–358.
11. Martin GV, Caldwell JH, Rasey JS, Grunbaum Z, Cerqueira M, Krohn KA. Enhanced binding of the hypoxic cell marker [^{3}H]fluoromisonidazole in ischemic myocardium. *J Nucl Med* 1989;30:194–201.
12. Martin GV, Cerqueira MD, Caldwell JH, Rasey JS, Embree L, Krohn KA. Fluoromisonidazole. A metabolic marker of myocyte hypoxia. *Circ Res* 1990;67:240–244.
13. Linder KE, Chan Y-W, Cyr JE, Malley MF, Nowotnik DP, Nunn AD. TcO(PnAO-1-(2-nitroimidazole)) [BMS-181321], a new technetium-containing nitroimidazole complex for imaging hypoxia: synthesis, characterization, and xanthine oxidase-catalyzed reduction. *J Med Chem* 1994;37:9–17.
14. Shi Q-X, Dione DP, Singer MJ, et al. Technetium-99m nitroimidazole: a positive imaging agent for the detection of myocardial ischemia [Abstract]. *Circulation* 1993;88:I–249.
15. Dahlberg ST, Gilmore MP, Flood M, Leppo JA. Effect of hypoxia and low-flow ischemia on the myocardial extraction of technetium-99m-nitroimidazole [Abstract]. *Circulation* 1993;88:I–250.
16. Connelly CM, Vogel WM, Hernandez YM, Apstein CS. Movement of necrotic wavefront after coronary occlusion in rabbit. *Am J Physiol* 1982;243:H682–H690.
17. Miura T, Downey JM, Ooiwa H, et al. Progression of myocardial infarction in a collateral flow deficient species. *Jpn Heart J* 1989;30:695–708.
18. Horneffer PPJ, Healy B, Gott VL, Gardner TJ. The rapid evolution of a myocardial infarction in an end-artery coronary preparation. *Circulation* 1987;76:V-39–V-42.

19. Reinhardt CP, Weinstein H, Leppo JA. Iodine-125-BMIPP as a marker of myocardial hypoperfusion: comparison to ^{201}Tl by quantitative dual tracer autoradiography and segmental tissue analysis. *J Nucl Med* 1995;36:1645–1653.
20. Chopra P, Sabherwal U. Histochemical and fluorescent techniques for detection of early myocardial ischemia following experimental coronary artery occlusion: a comparative and quantitative study. *Angiology* 1988;39:132–140.
21. Cox JL, McLaughlin VW, Flowers NC, Horan LG. The ischemic zone surrounding acute myocardial infarction. Its morphology as detected by dehydrogenase staining. *Am Heart J* 1968;76:650–659.
22. Shnitka TK, Nachlas MM. Histochemical alterations in ischemic heart muscle and early myocardial infarction. *Am J Pathol* 1963;42:507–527.
23. Reinhardt CP, Weinstein H, Wironen J, Leppo JA. Effect of triphenyl tetrazolium chloride staining on the distribution of radiolabeled pharmaceuticals. *J Nucl Med* 1993;34:1722–1727.
24. Hales JRS. Radioactive microsphere techniques for studies of the circulation. *Clin Exp Pharm Phys* 1974:31–46.
25. Heymann MA, Payne BD, Hoffman JIE, Rudolph AM. Blood flow measurement with radionuclide-labeled particles. *Prog Cardiovasc Dis* 1977;20:55–79.
26. Connelly CM, Leppo JA, Weitzman PW, Vogel WM, Apstein CS. Effect of coronary occlusion and reperfusion on myocardial blood flow during infarct healing. *Am J Physiol* 1989;257:H365–H374.
27. Whitmore GF, Varghese AJ. The biological properties of reduced nitroheterocyclics and possible underlying biochemical mechanisms. *Biochem Pharmacol* 1986;35:97–103.
28. Biaglow JE, Varnes ME, Roizen-Towle L, et al. Biochemistry of reduction of nitro heterocycles. *Biochem Pharmacol* 1986;35:77–90.
29. Koch CJ, Stobbe CC, Baer KA. Metabolism induced binding of ^{14}C-misonidazole to hypoxic cells: kinetic dependence on oxygen concentration and misonidazole concentration. *Intl J Radiat Oncol Biol Phys* 1984;10:1327–1331.
30. Franko AJ, Chapman JD, Koch CJ. Binding of misonidazole to EMT6 and V79 spheroids. *Intl J Radiat Oncol Biol Phys* 1982;8:737–739.
31. Kirsti Y, Liu Y, Tsuchida A, et al. Rat and rabbit heart infarction: effects of anesthesia, perfusate, risk zone, and method of infarct sizing. *Am J Physiol* 1994;267:H2383–H2390.
32. Martin GV, Biskupiak JE, Caldwell JH, Rasey JS, Krohn KA. Characterization of iodovinylmisonidazole as a marker for myocardial hypoxia. *J Nucl Med* 1993;34:918–924.
33. Martin GV, Caldwell JH, Graham MM, et al. Noninvasive detection of hypoxic myocardium using fluorine-18-fluoromisonidazole and positron emission tomography. *J Nucl Med* 1992;33:2202–2208.
34. Morguet AJ, Munz DL, Klein HH, et al. Myocardial distribution of indium-111-antimyosin Fab and technetium-99m-sestamibi in experimental nontransmural infarction. *J Nucl Med* 1992;33:223–228.
35. Shi CQ-X, Sinusas AJ, Dione DP, et al. Technetium-99m-nitroimidazole (BMS181321): a positive imaging agent for detecting myocardial ischemia. *J Nucl Med* 1995;36:1078–1086.
36. Hoffman JM, Rasey JS, Spence AM, Shaw DW, Krohn KA. Binding of the hypoxia tracer [^{3}H]misonidazole in cerebral ischemia. *Stroke* 1987;18:168–176.
37. Okada RD, Jacobs ML, Daggett WM, et al. Thallium-201 kinetics in nonischemic canine myocardium. *Circulation* 1982;65:70–77.
38. Eckelman WC. Diagnostic isotopes: prospects for improved agents. *Invest Radiol* 1989;24:252–254.